Fig. 5 Interacting peptides to Patched-1 (Ptch1) inhibited the interaction between Ptch1 and sonic hedgehog (*Shh*). AsPC1 cells were incubated with the peptides, A, B, C, and G as indicated. Then the cells were stained with Shh (*upper panels*). *Lower panels* show phase-contrast images (*Phase*) of peptides A, B, C, and G (*from left to right*). *Bars* 50 μm

Interacting peptides to Ptch1 suppressed pancreatic tumor growth in vivo

We confirmed the anti-cancer effect of peptides in vivo using AsPC1 cell xenografts. When the transplanted tumors had grown sufficiently to be palpable, peptide A or C was injected into the mice. The tumor size was measured every 2 days and the tumor volume was deduced from the measured data. The tumor volume was suppressed by peptide C in comparison to peptide A (Fig. 6a, b). The tumors were finally harvested and the Gli1 mRNA expression level was examined by RT-PCR. The Gli1 expression level of the tumor injected with peptide C was significantly reduced compared with that in the tumor injected with peptide A (Fig. 6c, d). To further confirm the in vivo effect of the synthesized peptides, SUIT2 was transplanted into mice and treated with peptide G or peptide A. Consistent with the results for AsPC1 and peptide C, Gli1 expression was significantly suppressed by peptide G in the SUIT2 xenograft.

Discussion

We have shown that peptides designed to interact with Ptch1 protein suppressed the activity of the Hh signaling pathway in pancreatic cancer cells, and suppressed the proliferation of pancreatic cancer cells. The anti-cancer effect of the peptides was further confirmed in vivo in a xenograft of the pancreatic cancer cell lines, AsPC1 and SUIT2. Finally, the mRNA expression of Gli1 in the xenograft was found to be reduced by the complementary peptides.

Three interacting peptides, B, C, and G, showed the same effect on both AsPC1 and SUIT2. However, peptide F showed a suppressive effect only on SUIT2, and the effect was reproducible. Recently, signal cross-talk between the Hh signaling pathway and Ras or p53 has been reported [24–30]. Both AsPC1 and SUIT2 have the same mutated amino acid sequence in Ras G12D [31]. However, they have different mutations in p53, as AsPC1 has a frame-shift mutation (135 TGC-GC), and SUIT2 has a point mutation (273 CGT-CAT) [31]. The different status of signals involved in cross-talk with the Hh signaling pathway may affect the response of pancreatic cancer cells to the interacting peptides to Ptch1.

Ptch1 is a unique receptor of the Hh signaling pathway. In the absence of ligand stimulation, Ptch1 suppresses Smo, an activating element of the Hh signaling pathway [32–36]. Our peptides were designed to interact with Ptch1. If the peptides interact with Ptch1 to suppress Ptch1 function, Smo and the Hh signaling pathway may be suppressed. We
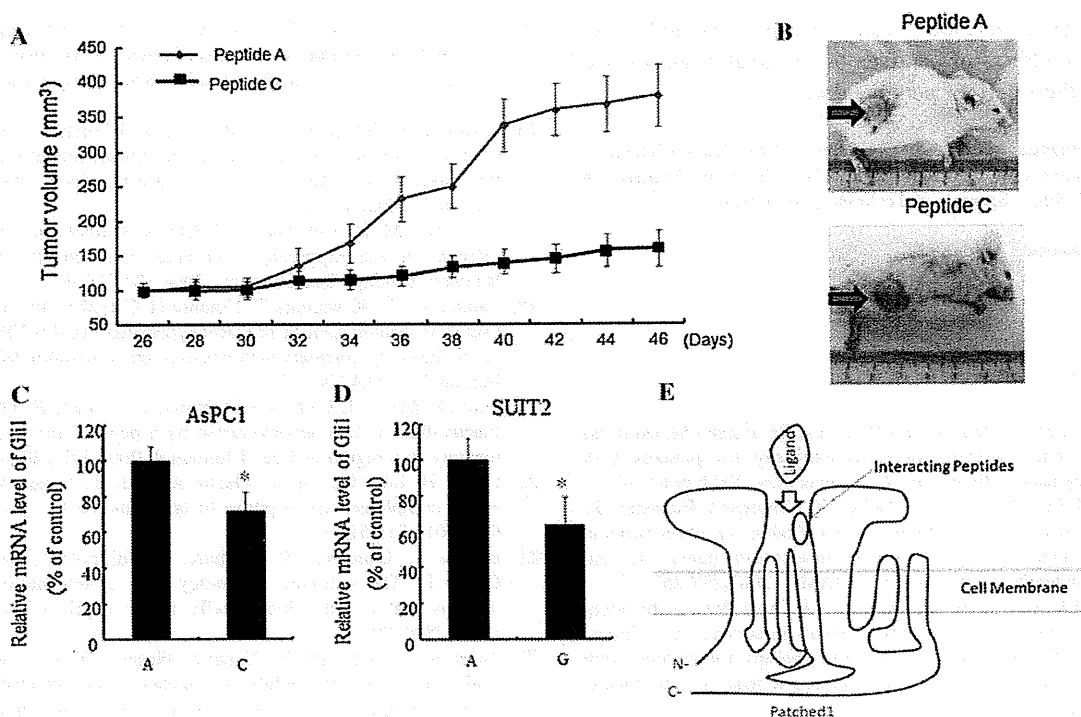
Fig. 6 Interacting peptides suppressed pancreatic tumor growth in vivo. AsPC1 tumor volume was suppressed by peptide C in comparison to peptide A (a). *Arrows* indicate implanted tumors (b). Gli1 expression in the tumor injected with peptide C was significantly decreased compared with that in the tumor injected with peptide A (c). In SUIT2 tumors, peptide G similarly reduced Gli1 expression

(d). Results are expressed as means ± SD. *$P < 0.05$. **e** Schema of the interacting peptide and Ptch1. The site of the interacting peptide corresponds to the target amino acid sequence of Ptch1. The schema indicates the putative mechanism, i. e., that the peptide interferes with the interaction between Ptch1 and the ligand of the Hh signaling pathway. *N* amino terminus, *C* carboxy terminus

aimed to suppress the activity of the Hh signaling pathway to control the proliferation of the pancreatic cancer cells. Thus, the target of the peptides was the short amino acid sequence of Ptch1 (KADYPNIQH) which was located in the putative docking site of the Hh ligand and Ptch1 (Fig. 6e) [37]. Furthermore, this Ptch1 sequence was previously selected for generating antibodies. As the site of the sequence was determined to be hydrophilic, the protein structure suggests it may not be folded inwards [37], and may enable peptides to access Ptch1 easily.

Controlling the Hh signaling pathway may contribute not only to controlling the proliferation of cancer cells, but also to controlling other significant events essential for carcinogenesis. For example, inhibition of the Hh signaling pathway has been shown to reduce the expression of the transcription factor snail, allowing the upregulation of E-cadherin, resulting in the inhibition of epithelial-to-mesenchymal transition and the reduction of in vitro invasive capacity [32]. Nagai et al. reported that blockade of the Hh pathway by cyclopamine inhibited pancreatic cancer cell invasion in association with the decreased expression of matrix metalloproteinase-9 [15]. These findings indicate that suppression of the Hh signaling

pathway may be a putative therapeutic method to suppress both tumor growth and tumor invasion.

The Hh signaling pathway was first reported to be reactivated in an autocrine signaling manner, although it originally functioned as a paracrine signal. Recently, several studies have added new knowledge of the paracrine networks of the Hh signaling pathway in cancer tissue. Olsen et al. reported that Hh-interacting protein was highly expressed in endothelial cells but was downregulated during angiogenesis and in several human tumors [38]. Guimaraes et al. [39] reported that Shh increased the mRNA levels of vascular endothelial growth factor, stromal cell-derived factor-1, and angiopoietin-1. Nakamura et al. [40] reported that pancreatic cancer cell-derived Shh induced angiotensin-1 and insulin-like growth factor-1 production in bone marrow-derived pro-angiogenic cells, resulting in their enhanced migration and capillary morphogenetic activity.

It is possible that the Hh signaling pathway is reactivated in pancreatic cancer and controls several kinds of cells in cancer tissue for cancer development, just as it is originally activated and controls several kinds of cells in fetal tissue [41]. The studies cited here highlight the significance of controlling the Hh signaling pathway in the

treatment of pancreatic cancer. Further research may improve the effects of peptides on pancreatic tumors and determine the safety of putative drugs.

Conflict of interest None.

References

1. Nakamura M, Wada J, Suzuki H, Tanaka M, Katano M, Morisaki T. Long-term outcome of immunotherapy for patients with refractory pancreatic cancer. Anticancer Res. 2009;29:831–6.

2. Oettle H, Post S, Neuhaus P, Gellert K, Langrehr J, Ridwelski K, et al. Adjuvant chemotherapy with gemcitabine vs. observation in patients undergoing curative-intent resection of pancreatic cancer: a randomized controlled trial. JAMA. 2007;297:267–77.

3. Burris HA 3rd, Moore MJ, Andersen J, Green MR, Rothenberg ML, Modiano MR, et al. Improvements in survival and clinical benefit with gemcitabine as first-line therapy for patients with advanced pancreas cancer: a randomized trial. J Clin Oncol. 1997;15:2403–13.

4. Nakamura M, Masuda H, Horii J, Kuma K, Yokoyama N, Ohba T, et al. When overexpressed, a novel centrosomal protein, RanBPM, causes ectopic microtubule nucleation similar to gamma-tubulin. J Cell Biol. 1998;143:1041–52.

5. Koorstra JB, Hustinx SR, Offerhaus GJ, Maitra A. Pancreatic carcinogenesis. Pancreatology. 2008;8:110–25.

6. Kameda C, Tanaka H, Yamasaki A, Nakamura M, Koga K, Sato N, et al. The Hedgehog pathway is a possible therapeutic target for patients with estrogen receptor-negative breast cancer. Anticancer Res. 2009;29:871–9.

7. Thayer SP, di Magliano MP, Heiser PW, Nielsen CM, Roberts DJ, Lauwers GY, et al. Hedgehog is an early and late mediator of pancreatic cancer tumorigenesis. Nature. 2003;425:851–6.

8. Berman DM, Karhadkar SS, Maitra A, Montes De Oca R, Gerstenblith MR, Briggs K, Beachy PA, et al. Widespread requirement for Hedgehog ligand stimulation in growth of digestive tract tumours. Nature. 2003;425:846–51.

9. Kubo M, Nakamura M, Tasaki A, Yamanaka N, Nakashima H, Nomura M, et al. Hedgehog signaling pathway is a new therapeutic target for patients with breast cancer. Cancer Res. 2004;64:6071–4.

10. Nakashima H, Nakamura M, Yamaguchi H, Yamanaka N, Akiyoshi T, Koga K, et al. Nuclear factor-kappaB contributes to hedgehog signaling pathway activation through sonic hedgehog induction in pancreatic cancer. Cancer Res. 2006;66:7041–9.

11. Yanai K, Nagai S, Wada J, Yamanaka N, Nakamura M, Torata N, et al. Hedgehog signaling pathway is a possible therapeutic target for gastric cancer. J Surg Oncol. 2007;95:55–62.

12. Kameda C, Nakamura M, Tanaka H, Yamasaki A, Kubo M, Tanaka M, et al. Oestrogen receptor-alpha contributes to the regulation of the hedgehog signalling pathway in ER alpha-positive gastric cancer. Br J Cancer. 2010;102:738–47.

13. Nakamura M, Kubo M, Yanai K, Mikami Y, Ikebe M, Nagai S, et al. Anti-patched-1 antibodies suppress hedgehog signaling pathway and pancreatic cancer proliferation. Anticancer Res. 2007;27:3743–7.

14. Koga K, Nakamura M, Nakashima H, Akiyoshi T, Kubo M, Sato N, et al. Novel link between estrogen receptor alpha and hedgehog pathway in breast cancer. Anticancer Res. 2008;28:731–40.

15. Nagai S, Nakamura M, Yanai K, Wada J, Akiyoshi T, Nakashima H, et al. Gli1 contributes to the invasiveness of pancreatic cancer through matrix metalloproteinase-9 activation. Cancer Sci. 2008;99:1377–84.

16. Campbell W, Kleiman L, Barany L, Li Z, Khorchid A, Fujita E, et al. A novel genetic algorithm for designing mimetic peptides that interfere with the function of a target molecule. Microbiol Immunol. 2002;46:211–5.

17. Hosokawa M, Imai M, Okada H, Okada N. Inhibition of HIV-1 infection in cells expressing an artificial complementary peptide. Biochem Biophys Res Commun. 2004;324:236–40.

18. Shimomura Y, Kawamura T, Komura H, Campbell W, Okada N, Okada H. Modulation of procarboxypeptidase R (ProCPR) activation by complementary peptides to thrombomodulin. Microbiol Immunol. 2003;47:241–5.

19. Fujita E, Farkas I, Campbell W, Baranyi L, Okada H, Okada N. Inactivation of C5a anaphylatoxin by a peptide that is complementary to a region of C5a. J Immunol. 2004;172:6382–7.

20. Okada H, Imai M, Ono F, Okada A, Tada T, Mizue Y, et al. Novel complementary peptides to target molecules. Anticancer Res. 2011;31:2511–6.

21. Baranyi L, Campbell W, Ohshima K, Fujimoto S, Boros M, Okada H. The antisense homology box: a new motif within proteins that encodes biologically active peptides. Nat Med. 1995;1:894–901.

22. Akiyoshi T, Nakamura M, Yanai K, Nagai S, Wada J, Koga K, et al. Gamma-secretase inhibitors enhance taxane-induced mitotic arrest and apoptosis in colon cancer cells. Gastroenterology. 2008;134:131–44.

23. Nakamura M, Zhou XZ, Kishi S, Lu KP. Involvement of the telomeric protein Pin2/TRF1 in the regulation of the mitotic spindle. FEBS Lett. 2002;514:193–8.

24. Lauth M, Bergstrom A, Shimokawa T, Tostar U, Jin Q, Fendrich V, et al. DYRK1B-dependent autocrine-to-paracrine shift of Hedgehog signaling by mutant RAS. Nat Struct Mol Biol. 2010;17:718–25.

25. Nolan-Stevaux O, Lau J, Truitt ML, Chu GC, Hebrok M, Fernandez-Zapico ME, Hanahan D. GLI1 is regulated through Smoothened-independent mechanisms in neoplastic pancreatic ducts and mediates PDAC cell survival and transformation. Genes Dev. 2009;23:24–36.

26. Stecca B, Mas C, Clement V, Zbinden M, Correa R, Piguet V, et al. Melanomas require HEDGEHOG-GLI signaling regulated by interactions between GLI1 and the RAS-MEK/AKT pathways. Proc Natl Acad Sci USA. 2007;104:5895–900.

27. Ji Z, Mei FC, Xie J, Cheng X. Oncogenic KRAS activates hedgehog signaling pathway in pancreatic cancer cells. J Biol Chem. 2007;282:14048–55.

28. Abe Y, Oda-Sato E, Tobiume K, Kawauchi K, Taya Y, Okamoto K, et al. Hedgehog signaling overrides p53-mediated tumor suppression by activating Mdm2. Proc Natl Acad Sci USA. 2008;105:4838–43.

29. Katoh Y, Katoh M. Integrative genomic analyses on GLI2: mechanism of Hedgehog priming through basal GLI2 expression, and interaction map of stem cell signaling network with P53. Int J Oncol. 2008;33:881–6.

30. Stecca B, Ruiz i Altaba A. A GLI1-p53 inhibitory loop controls neural stem cell and tumour cell numbers. EMBO J. 2009;28:663–76.

31. Moore PS, Sipos B, Orlandini S, Sorio C, Real FX, Lemoine NR, et al. Genetic profile of 22 pancreatic carcinoma cell lines. Analysis of K-ras, p53, p16 and DPC4/Smad4. Virchows Arch. 2001;439:798–802.

32. Feldmann G, Dhara S, Fendrich V, Bedja D, Beaty R, Mullendore M, et al. Blockade of hedgehog signaling inhibits pancreatic cancer invasion and metastases: a new paradigm for combination therapy in solid cancers. Cancer Res. 2007;67:2187–96.

33. Ingham PW, Nystedt S, Nakano Y, Brown W, Stark D, van den Heuvel M, Taylor AM. Patched represses the Hedgehog signalling pathway by promoting modification of the Smoothened protein. Curr Biol. 2000;10:1315–8.

34. Pepinsky RB, Rayhorn P, Day ES, Dergay A, Williams KP, Galdes A, et al. Mapping sonic hedgehog-receptor interactions by steric interference. J Biol Chem. 2000;275:10995–1001.

35. Martin V, Carrillo G, Torroja C, Guerrero I. The sterol-sensing domain of Patched protein seems to control Smoothened activity through Patched vesicular trafficking. Curr Biol. 2001;11:601–7.

36. Stone DM, Hynes M, Armanini M, Swanson TA, Gu Q, Johnson RL, et al. The tumour-suppressor gene patched encodes a candidate receptor for Sonic hedgehog. Nature. 1996;384:129–34.

37. Goodrich LV, Johnson RL, Milenkovic L, McMahon JA, Scott MP. Conservation of the hedgehog/patched signaling pathway from flies to mice: induction of a mouse patched gene by Hedgehog. Genes Dev. 1996;10:301–12.

38. Olsen CL, Hsu PP, Glienke J, Rubanyi GM, Brooks AR. Hedgehog-interacting protein is highly expressed in endothelial cells but down-regulated during angiogenesis and in several human tumors. BMC Cancer. 2004;4:43.

39. Guimaraes AR, Rakhlin E, Weissleder R, Thayer SP. Magnetic resonance imaging monitors physiological changes with anti-hedgehog therapy in pancreatic adenocarcinoma xenograft model. Pancreas. 2008;37:440–4.

40. Nakamura K, Sasajima J, Mizukami Y, Sugiyama Y, Yamazaki M, Fujii R, et al. Hedgehog promotes neovascularization in pancreatic cancers by regulating Ang-1 and IGF-1 expression in bone-marrow derived pro-angiogenic cells. PLoS One. 2010;5:e8824.

41. van den Brink GR, Bleuming SA, Hardwick JC, Schepman BL, Offerhaus GJ, Keller JJ, et al. Indian Hedgehog is an antagonist of Wnt signaling in colonic epithelial cell differentiation. Nat Genet. 2004;36:277–82.

HMGB1 release by C5a anaphylatoxin is an effective target for sepsis treatment

Noriko Okada*, Masaki Imai*, Alan Okada[&], Fumiko Ono[#] and Hidechika

Okada*,[&]

*Department of Immunology, Nagoya City University Graduate School of Medical

Sciences, Nagoya 467-8601, [&]Choju Medical Institute, Fukushimura Hospital,

Toyohashi 411-8124, and [#]Tsukuba Primate Research Center, National Institute of

Biomedical Innovation, Tsukuba 305-0843, Japan

Address correspondence and reprint request to Dr. Hidechika Okada, Choju Medical

Institute, Fukushimura Hospital, Noyori-cho, Yamanaka 19-14, Toyohashi 441-8124,

Japan E-mail: hiokada@med.nagoya-cu.ac.jp

Key words: complement; C5a; anaphylatoxin; inflammation; sepsis; peptide; endotoxin-

shock; C5a receptor; C5L2; HMGB1; cytokine storm.

1

Antibodies to C5a have proven to be effective in treating experimental septic primate models[1,2]. A 17 amino acid peptide (ASGAPAPGPAGPLRPMF) named PepA binds to C5a and prevents complement-mediated lethal shock in rats[3].

AcPepA harboring an acetyl group at the N-terminal alanine showed increased inhibitory activity against C5a[4]. Cynomolgus monkeys destined to expire from a lethal dose of bacterial endotoxin (4mg/kg) were rescued by intravenous administration of AcPepA. AcPepA could have interfered with the ability of C5a to stimulate C5L2[5,6] which is responsible for HMGB1 release and stimulation of TLR4[7-9] as an endogeneous ligand with LPS behavior. The suppression of HMGB1 release by AcPepA administration to LPS-shock monkeys is likely responsible for rescuing the animals.

Sepsis is a systemic inflammatory response syndrome (SIRS) that causes disseminated intravascular coagulation (DIC) and multiple organ failure (MOF).

Antibodies to C5a have proven to be effective in treating experimental septic primate models[1,2]. We generated an inhibitory peptide of C5a composed of an amino acid sequence ASGAPAPGPAGPLRPMF named PepA[3]. Acetylation at the N-terminal alanine of PepA improved the C5a inhibitory capacity and was named AcPepA[4].

Under anesthesia with sodium pentobarbital, 10 cynomolgus monkeys (weighing about 5 kg) were intravenously administered 4 mg/kg LPS within 30 min. Three monkeys for the control group were infused with 15 ml saline during 3 hrs after the LPS injection. Seven experimental group monkeys were infused intravenously with 15 ml of 2 mg/ml AcPepA starting at 30 min after LPS injection for 3 hrs (2 mg/kg/hr for 3 hrs). Six hrs after LPS administration, anesthesia was terminated when the blood samples showed leukocytosis and increased CPK in all monkeys. Monkeys were observed for their status. All of the 7 AcPepA treated monkeys returned to a healthy condition by the following day, while the 3 control monkeys died within two days.

Despite the increased TNFα and other cytokine levels, high mobility group box 1 (HMGB1)[5,6] which is an endogenous stimulator of TLR4[7-9] did not increase in the AcPepA infused animals (Fig. 1).

Furthermore, AcPepA could suppress pathophysiological events and prolonged survival time of sepsis piglets induced by cecal ligation and perforation (CLP)[10]. Survival times were longer in the AcPepA treated group than in the CLP alone group (19.3hrs ± 2.7hrs vs. 9.9 hrs ± 0.7 hrs, $P<0.005$). In this case, AcPepA also delayed the HMGB-1 surge.

These above results indicate that suppression of C5 anaphylatoxin interferes with

3

the induction of a cytokine storm. Since C5a has the capacity to cause release of HMGB1 following stimulation of the second C5a receptor termed C5L2 generated on activated monocytes[11-13], inhibition of C5a successfully interferes with the above release which has the capacity to generate inflammatory cytokines stimulating TLR4 as an endogenous ligand (Fig. 2).

Recently, thrombomodulin (TM) administration has been shown to rescue septic shock animals[14]. The enhanced activity of thrombin when complexed with TM should have caused activation of thrombin activatable fibrinolysis inhibitor (TAFI) which then inactivates C5a anaphylatoxin by removing the C-terminal arginine[15,16] resulting in suppression of HMGB1 release. Therefore, the therapeutic effect of TM on sepsis should also be due to inactivation of C5a anaphylatoxin which initiates a cytokine storm through HMGB1 release.

References

4

1. Czermak, B.J., V. Sarma, C. L. Pierson, R. L. Warner, M. Huber-Lang, N. M. Bless, H. Schmal, H. P. Friedl, and P. A. Ward, 1999. Protective effects of C5a blockade in sepsis. *Nature.Med.* **5**: 788-792.

2. Stevens, J.H., P. O'Hanley, J.M. Shapiro, F.G. Mihm, P.S. Satoh, J.A. Collins, and T.A. Raffin. 1986. Effects of anti-C5a antibodies on the adult respiratory distress syndrome in septic primates. *J. Clin. Invest.* **77**: 1812-1816.

3. Fujita, E., I. Farkas, W. Campbell, L. Baranyi, H. Okada, and N. Okada. 2004. Inactivation of C5a anaphylatoxin by a peptide that is complementary to a region of C5a. *J. Immunol.* **172**: 6382-6387.

4. Okada, N., S. Asai, A. Hotta, N. Miura, N. Ohno, I. Farkas, L. Hau, and H. Okada. 2007. Increased inhibitory capacity of an anti-C5a complementary peptide following acetylation of N-terminal alanine. *Microbiol. Immunol.* **51**: 439-443.

5. Wang, H., O. Bloom, M. Zhang, J.M. Vishnubhakat, M. Ombrellino, J. Che, A. ., Frazier, H. Yang, S. Ivanova, L. Borovikova, K.R. Manogue, E. Faist, E. Abraham, J. Andersson, U. Andersson, P.E. Molina, N.N. Abumrad, A. Sama, and K.J. Tracey. 1999. HMGB-1 as a late mediator of endotoxin lethality in mice. *Science* **285**: 248-251.

6. Riedemann NC, R-F. Guo RF, and P.A. Ward. 2003. Novel strategies for the treatment of sepsis. *Nature. Med.* **9**: 517-524.

7. Yu, M., H. Wang, A. Ding, D.T. Golenbock, E. Latz, C.J. Czura, M.J. Fenton, K.J. Tracey, H. Yang. 2006. HMGB1 signals through toll-like receptor (TLR) 4 and TLR2. *Shock* **26**: 174-179.

8. Yang, H., M. Ochani, J. Li, X. Qiang, M. Tanovic, H. Harris, S.M. Susaria, M.P. Ulloa, H. Wang, R. DiRimo, C.J. Czura, H.Wang, J. Roth, H.S. Warren, H.S., M.P. Fink, M.J. Fenton, U. Andersson, and K.J. Tracey. 2004. Reversing established sepsis with antagonists of endogeneous high-mobility group box 1. *Proc. Natl. Acad. Sci.* **101**: 296-301.

9. Park, J.S., F. Gamboni-Robertson, Q. He, D. Svetkauskaite, J.Y. Kim, D. Strassheim, J.W. Sohn, S. Yamada, I. Maruyama, A. Banerjee, A. Ishizaka, and E. Abraham, E. 2006. High mobility group box 1 protein interacts with multiple Toll-like receptors. *Am. J. Physiol. Cell. Physiol.* **290**: C917-924.

10. Hussein, MH., Kato, S., Goto, T., Daoud, GA., Kato, I., Suzuki, S., Togari, H., Imai, M., Okada, N., Okada, H. An acetylated anti-C5a complementary peptide reduced cytokines and free radicals and prolongs survival time in a neonatal sepsis model **Mol Immunol** 2009, 46:2825

11. Chen, N-J., Mirtsos, C., Suh, D., Lu, Y-C., Lin, W-J., McKerlie, C., Lee, T., Baribault, H., Tian, H. and Yeh, W-C. 2007. C5L2 is critical for the biological activities of the anaphylatoxins C5a and C3a. *Nature* 446: 203-207.

12. Klune, J.R., Dhupar, R., Cardinal, J., Billiar, T.R. and Tsung, A. 2008. HMGB1:endogeneous danger signaling. Mol. Med. 14:476-484.

13. Rittirsch, D., Flierl, M.A., Nadeau, B.A., Day, D.E., Huber-Lang, M., Mackay, C.R., Zetoune, F.S., Gerard, N.P., Cianflone, K., Koehl, J., Gerard, C., Sarma, J.V. and Ward, P.A. 2008. Functional roles for C5a receptors in sepsis. *Nature Med.* **14**: 551-557.

14. Nagato M, Okamoto K, Abe Y, Higure A, Yamaguchi K. 2009. Recombinant human soluble thrombomodulin decreases the plasma high-mobility group box-1 protein

levels, whereas improving the acute liver injury and survival rates in experimental

endotoxemia. *Crit Care Med.* **37**::2181-2186.

15. Campbell, W., N. Okada, and H. Okada. 2001. Carboxypeptidase R (CPR) is an
    inactivator of complement derived inflammatory peptides and an inhibitor of
    fibrinolysis. *Immunol. Rev.* **180**: 162-167.

16. Campbell, W., E. Lazoura, N. Okada, and H. Okada. 2002. Inactivation of C3a and
    C5a octapeptides by carboxypeptidase R and carboxypeptidase N. *Microbiol.
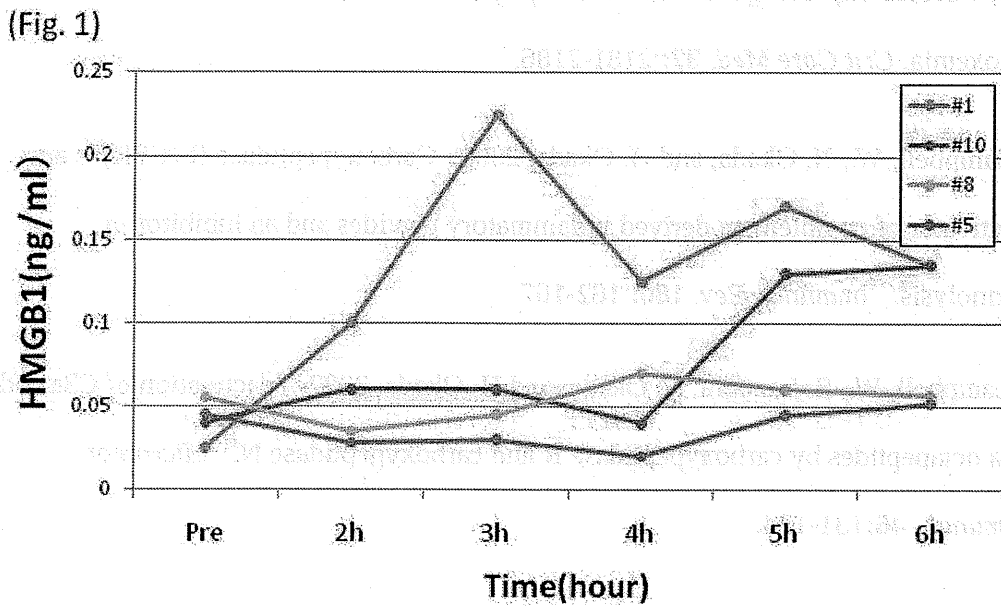   Immunol.* **46**:131-134.

(Fig. 1)

Figure 1. Increase in HMGB1 in plasma of LPS- injected monkeys.

Six cynomolgus monkeys intravenously infused with a lethal dose of bacterial LPS

(4mg/kg) destined to death were treated with intravenous administration of 2 mg/kg/h of

AcPepA for 3h starting 30 min after the lethal LPS injection (#5 and #8).. Control

monkeys (#1 and #10) were infused only saline in stead of AcPepA following LPS

injection. Despite the increased TNFα and other cytokine levels, high mobility group

box 1 (HMGB1) which is an endogenous stimulator of TLR4[7] did not increase in the

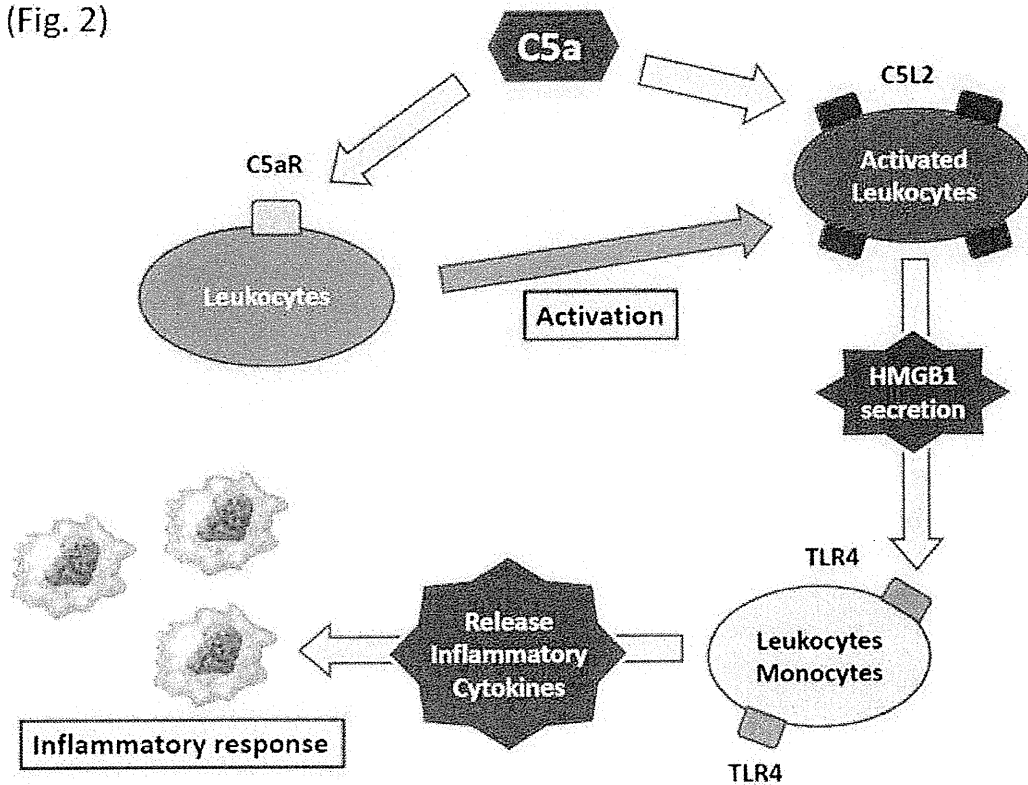AcPepA infused animals (#5 and #8).

8

(Fig. 2)

Figure 2. Possible role for C5a in a positive feedback inflammatory circuit.

Following bacterial infection, LPS stimulates TLR4, and C5a generated during

complement activation stimulates C5aR resulting in expression of C5L2 on leukocyte

membranes. Stimulation of C5L2 by C5a on activated leukocytes induces release of

HMGB1 which then reacts with TLR-4 on other leukocytes, as did LPS, resulting in

further recruitment of activated leukocytes that express C5L2. These reactions create an

inflammatory amplification circuit.

Dominant Mutations in *RP1L1* Are Responsible for Occult Macular Dystrophy

Masakazu Akahori,[1] Kazushige Tsunoda,[1] Yozo Miyake,[1,2] Yoko Fukuda,[3] Hiroyuki Ishiura,[3] Shoji Tsuji,[3] Tomoaki Usui,[4] Tetsuhisa Hatase,[4] Makoto Nakamura,[5] Hisao Ohde,[6] Takeshi Itabashi,[1] Haru Okamoto,[1] Yuichiro Takada,[1] and Takeshi Iwata[1,*]

Occult macular dystrophy (OMD) is an inherited macular dystrophy characterized by progressive loss of macular function but normal ophthalmoscopic appearance. Typical OMD is characterized by a central cone dysfunction leading to a loss of vision despite normal ophthalmoscopic appearance, normal fluorescein angiography, and normal full-field electroretinogram (ERGs), but the amplitudes of the focal macular ERGs and multifocal ERGs are significantly reduced at the central retina. Linkage analysis of two OMD families was performed by the SNP High Throughput Linkage analysis system (SNP HiTLink), localizing the disease locus to chromosome 8p22-p23. Among the 128 genes in the linkage region, 22 genes were expressed in the retina, and four candidate genes were selected. No mutations were found in the first three candidate genes, methionine sulfoxide reductase A (*MSRA*), GATA binding 4 (*GATA4*), and pericentriolar material 1 (*PCM1*). However, amino acid substitution of p.Arg45Trp in retinitis pigmentosa 1-like 1 (*RP1L1*) was found in three OMD families and p.Trp960Arg in a remaining OMD family. These two mutations were detected in all affected individuals but in none of the 876 controls. Immunohistochemistry of RP1L1 in the retina section of cynomolgus monkey revealed expression in the rod and cone photoreceptor, supporting a role of RP1L1 in the photoreceptors that, when disrupted by mutation, leads to OMD. Identification of *RP1L1* mutations as causative for OMD has potentially broader implications for understanding the differential cone photoreceptor functions in the fovea and the peripheral retina.

Occult macular dystrophy (OMD) is an autosomal-dominant form of inherited macular dystrophy characterized by progressive decrease of visual acuity due to macular dysfunction, which was first reported by Y.M. et al. in 1989.[1-3] The disorder was called "occult" because of the fact that the macular dysfunction of this disease is hidden by a normal fundus appearance. Typical OMD, as described by Y.M. et al., is characterized by central cone dysfunction and in some cases rod dysfunction, leading to a loss of vision despite normal ophthalmoscopic appearance, normal fluorescein angiography, and normal full-field electroretinograms (ERGs). However, the amplitudes of the focal macular ERGs and multifocal ERGs are significantly reduced, indicating dysfunction of the central retina.[1,2,4] OMD is known for its broad range of age at disease onset, from 6 to 81 yrs. Brockhurst et al. have reported age at onset of four out of eight OMD patients at over 65 yrs[5] and similar findings have also been observed in earlier cases.[1,2] The patient III-3 in family 1 did not notice any visual disturbance in her right eye even at the age of 81 yrs.

The four families shown in Figure 1 demonstrate dominant inheritance of the OMD phenotype. None of the patients had ocular diseases other than OMD, except senile cataract or diabetic retinopathy. Control family members were confirmed to be normal via a complete ophthalmic examination including focal macular ERGs or multifocal ERGs. For this study, the ethics review committees of the National Hospital Organization Tokyo Medical Center, the Niigata University Graduate School of Medical and Dental Sciences, and the Nagoya University Medical School approved the study, and written informed consent was obtained from both affected and unaffected subjects.

Linkage analysis of OMD families 1 and 2 was performed. Eighteen individuals from family 1 and eleven individuals from family 2 were genotyped by Affymetrix's Genome-Wide Human SNP array 6.0 in accordance with the manufacturer's instructions (Affymetrix, Santa Clara, CA). DNA samples from family 2 were subjected to whole-genome amplification with the use of REPLI-g (QIAGEN, Tokyo, Japan) prior to SNP genotyping. With SNP HiTLink[6] used as a pipeline, SNPs with a Hardy-Weinberg p value > f 0.001, a call rate of 1, and a maximum confidence score > 0.02 were used for the analysis. SNPs with the minor allele frequency of 0 in controls were eliminated from the analysis. Parametric multipoint linkage analysis (autosomal-dominant model with a setting of liability classes; age-dependent penetrance of 0.19, 0.55, and 0.91 for 0–20, 21–40, and > 41 yrs old, respectively, and disease frequency of 0.000001) was performed with Allegro version 2,[7] intermarker distance from 80 kb to 120 kb with the use of SNP HiTLink. Because of the limitation of computational capacity, family 1 was divided into two branches (branch 1-1: descendants of II-1; branch

A

I. Family 1

II.

III.

IV.

V.

Family 2   Family 3   Family 4

I.

II.

III.

○ Unaffected
◑ Vision abnormality
● Affected (ERG tested)
◉ Obligate gene carrier
n* Sample collected

B

R45W

G D P R>W F A G
AGGGGATCCA[Y]GGTTTGCTGG

affected

G D P R F A G
AGGGGATCCACGGTTTGCTGG

unaffected

W960R

V R E W>R L D N
GGTCCGCGAA[Y]GGCTGGACAA

affected

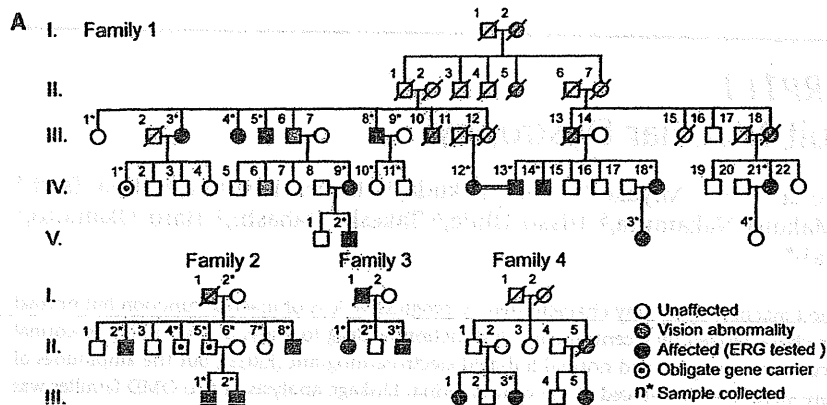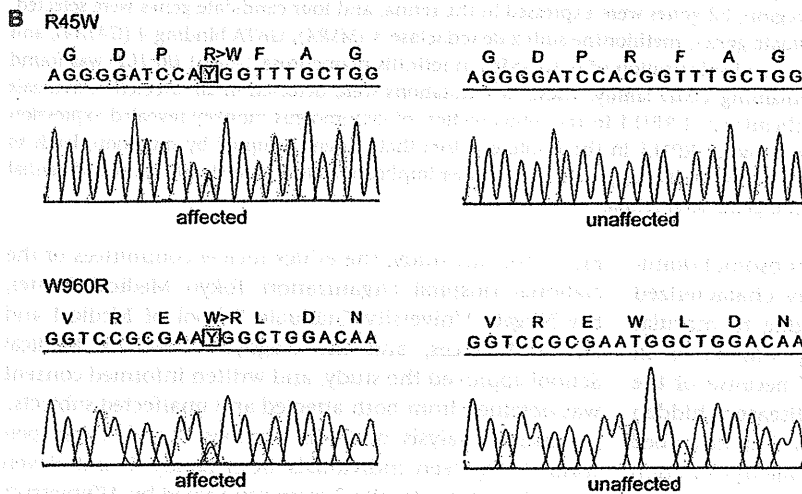V R E W L D N
GGTCCGCGAATGGCTGGACAA

unaffected

Figure 1. Autosomal OMD Families and DNA Sequencing of RP1L1

(A) The four families shown demonstrate dominant inheritance of the OMD phenotype. In all presented families, none of the patients had ocular diseases other than OMD, except senile cataract and diabetic retinopathy. Control family members were confirmed to be normal via a complete ophthalmic examination including focal macular ERGs or multifocal ERGs.

(B) DNA sequencing of both p.Arg45Trp and p.Trp960Arg mutations found in four independent families.

1-2: descendants of II-7) for multipoint linkage analysis. Haplotypes were reconstructed by Allegro.

The parametric linkage study of family 1 using SNP microarrays and SNP HiTLink mapped the disease locus to an approximately 10 Mb region of chromosome 8p22-p23 with a maximum LOD score of 3.77 (Figure 2). Parametric linkage analysis of affected individuals only produced similar results (Figure 3 and Figure S2 available online). A common haplotype between rs365309 and rs2632841 was shared by all of the affected individuals (Table 1). With the additional linkage study of family 2, the cumulative parametric multipoint LOD score rose to over 4 (Figure S1). A total of 128 known genes were found within the approximately 10 Mb linkage-associated region, containing 22 retina-expressed genes as candidates for mutational analyses. No mutations were found in the first three candidate genes, methionine sulfoxide reductase A (MSRA), GATA binding 4 (GATA4), and pericentriolar material 1 (PCM1). However, a c.362C>T (p.Arg45Trp) substitution in retinitis pigmentosa 1-like 1 (RP1L1 [MIM 608581]) was found in all affected individuals in family 1. We further extended the mutational analysis of RP1L1 to three other families with autosomal OMD, and we identified the p.Arg45Trp alteration in families 2 and 4 and

a c.3107T>C (p.Trp960Arg) mutation in family 3 (Table 2). Additionally, known and unknown natural variants were found in RP1L1, as shown in Table S2. Unknown SNPs were submitted to the dbSNP database.

In these four families, all of the affected individuals carried one of the two mutations identified in this study, c.362C>T or c.3107T>C. We identified three apparently unaffected individuals carrying the p.Arg45Trp mutation, which suggest a reduced penetrance of the mutation or possibility a later onset of the disease for these individuals. Both mutations were absent in 1752 Japanese control chromosomes.

Immunohistochemistry of RP1L1 in the macula section of primate Cynomolgus monkeys (Macaca fascicularis) was performed. The eyes from a 6-yr-old normal male cynomolgus monkey were obtained from Tsukuba Primate Research Center, National Institute of Biomedical Innovation, Japan. All experimental procedures were approved by the Animal Welfare and Animal Care Committee of the National Institute of Biomedical Innovation, in compliance with guidelines of the Association for Research in Vision and Ophthalmology. Cynomolgus eyes were removed and immediately fixed overnight with 4% paraformaldehyde in 0.1 M phosphate buffer, pH 7.4. After washing in PBS, eyes were cryoprotected in the gradient sucrose dissolved in PBS and embedded into optimal cutting temperature (OCT) compound (Tissue Tek, Miles, IL, USA). Frozen retinal sections cut at 8 μm thickness with cryostat were incubated at 4°C with a 1:500 dilution of human RP1L1 polyclonal antibody raised against the N terminus of human RP1L1 (Santa Cruz Biotechnology, Santa Cruz, CA, USA). Immunofluorescence was visualized with Alexa 568 goat anti-rabbit IgG (Invitrogen, Carlsbad, CA, USA), Alexa 488 PNA (Invitrogen) for detection of cone photoreceptor, and DAPI (Invitrogen) for nuclear staining. Fluorescence images were analyzed with a confocal laser
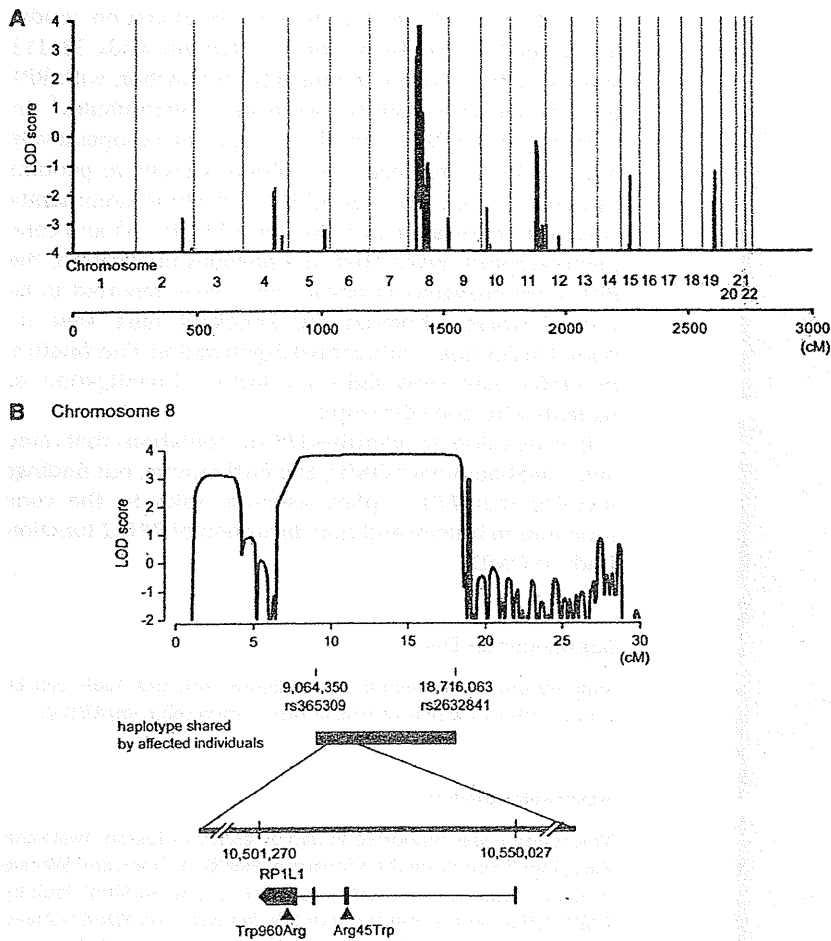
A

LOD score (axis labels 4, 3, 2, 1, 0, -1, -2, -3, -4)

Chromosome
1 2 3 4 5 6 7 8 9 10 11 12 13 14 15 16 17 18 19 21
                                                              20 22

0   500   1000   1500   2000   2500   3000
                                                                      (cM)

B Chromosome 8

LOD score (axis labels 4, 3, 2, 1, 0, -1, -2)

0   5   10   15   20   25   30
                                                          (cM)

9,064,350   18,716,063
rs365309   rs2632841

haplotype shared
by affected individuals

10,501,270   10,550,027
RP1L1

Trp960Arg   Arg45Trp

Figure 2. Linkage Analysis and Haplotype Analysis of Family 1

(A) Parametric multipoint linkage analysis of family 1. Horizontal axis indicates cumulative position (cM) from the short arm of chromosome 1. As a result of computational capacity, family 1 was divided into two branches for calculation of LOD scores. No other chromosomes except chromosome 8 yielded a positive LOD score.

(B) Parametric multipoint linkage analysis of family 1 and mutations in RP1L1. A maximum LOD score of 3.77 was obtained at 8p32.1-8p22. A haplotype bounded by rs365309 (physical position: 9,064,350 in the hg18 assembly of the UCSC Genome Browser) and rs2632841 (18,716,063) was shared by all affected individuals. Horizontal axis indicates the position (cM) on the short arm of chromosome 8. Vertical axis indicates the parametric multipoint LOD score. Mutations (p.Arg45Trp and p.Trp960Arg) are demonstrated.

microscope (Radiance 2000, Bio-Rad Laboratories, Hercules, CA, USA).

To our surprise, the immunohistochemistry of RP1L1 in the macula section of Cynomolgus monkeys revealed expression in retinal rod and cone photoreceptors by human RP1L1 antibody (Figure 3). This expression pattern is significantly different from the previous study of mouse RP1L1, in which RP1L1 was localized exclusively in axoneme of rods.[8] Furthermore, the human amino acid sequence is only 39% identical to that of the mouse, due to a lack of both polymorphic 16 amino acid repeats or a lack of the highly repetitive Glu-rich region, making mouse RP1L1 protein considerably shorter than the human protein, which may lead to different functional roles in the primate retina. Recent investigation of photoreceptor structure in OMD patients using advanced optical coherence tomography suggests that the predominant defect involves the cone photoreceptor.[9,10] Our optical coherence tomography observations also show loss of the cone outer segment tip and irregularity of the inner segment/outer segment junction in the center of the macula of all examined case individuals in family 1 (data not shown). Y.M. et al. have observed that not only cone but also rod sensitivity in the macula was abnormal in some of the older

patients.[1,2] It is likely that the initial event may be macular cone specific but may later extend to rod abnormality. Further investigation of RP1L1 function is required in order to answer these clinical observations.

RP1L1 was originally cloned as a gene derived from common ancestor as retinitis pigmentosa 1 (RP1 [MIM 180100]) on the same chromosome 8.[11,12] RP1L1 shares 35% amino acid identity with RP1, a gene responsible for 5%–10% of autosomal-dominant retinitis pigmentosa (RP [MIM 268000]) worldwide.[13–15] When RP1L1 was first identified, a number of attempts were made to identify mutations in RP1L1 in various RP patients, with no success. The present study demonstrates that RP1L1 mutation is responsible for OMD, but not for RP. Patients with RP carrying the most common RP1 alteration, p.Arg677X, exhibit night and peripheral vision disturbance beginning in the third decade of life. RP1 is found exclusively in the retina and is localized to both rods and cones. Rod-cone functional comparison in RP patients has indicated that rod sensitivity loss is at least 2 log units greater than cone sensitivity loss.[13] Thus phenotypic characteristics of RP caused by RP1 mutations and those of OMD caused by RP1L1 mutations perfectly agree with the different localizations of RP1 and RP1L1 in retina.

The outer segments of rod and cone photoreceptors are highly specialized cilia containing hundreds of disc membranes stacked in an orderly array along the photoreceptor axoneme. Previous studies have shown that RP1 is part of the axoneme and is required for this correct orientation and higher-order stacking of outer segment discs.[16] This is achieved by the interaction of RP1 with the
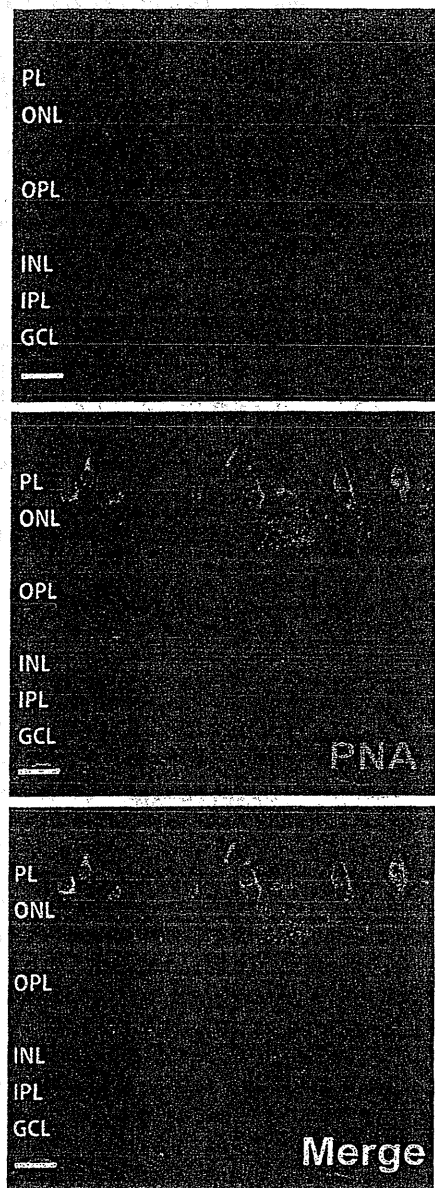
Figure 3. Immunohistochemistry of RP1L1 in the Cynomolgus Monkey Retina
Localization of RP1L1 in the rod and cone photoreceptors in the Cynomolgus monkey (*Macaca fascicularis*). Retina labeled with anti-human RP1L1 (red, top); same section labeled with retinal cone specific marker, peanut agglutinin lectin (PNA, green, middle); merged image (bottom). Yellow signal present in cone photoreceptor resulted from combination of the red signal of RP1L1 and the green signal of PNA. Cell nuclei were stained with DAPI (blue). PL, photoreceptor layer; ONL, outer nuclear layer; OPL, outer plexiform layer; INL, inner nuclear layer; IPL, inner plexiform layer; GCL, ganglion cell layer, Scale bars represent 20 μm.

microtubule in the connecting cilia.[17] RP1 contains microtubule-binding domains (amino acids 28–228) of neuronal microtubule-associated protein (MAP) doublecortin (DCX), which is required to maintain axoneme length

and stability.[18] The RP1L1 p.Arg45Trp alteration resides in one of the two DCX domains (amino acids 33–113 and 147–228), which is required for interaction with RP1 to assemble and stabilize axonemal microtubules.[8] In primates, both RP1L1 and RP1 proteins may cooperatively function in the rod and cone photoreceptors to perform this task. The mutation in *RP1L1* is likely to dominantly affect the cooperative function with RP1 in rod and cone photoreceptors, given that in a previous publication, the *RP1L1* heterozygous knockout mice were reported to be normal whereas homozygous knockout mice were reported to develop subtle retinal degeneration. Our findings in OMD may shed light for further investigation of patients with cone dystrophy.

In conclusion, we identified *RP1L1* mutations that cause autosomal-dominant OMD, and furthermore, our findings revealed that *RP1L1* plays essential roles in the cone functions in human and that disruption of *RP1L1* function leads to OMD.

Supplemental Data

Supplemental Data include three figures and one table can be found with this article online at http://www.cell.com/AJHG/.

Web Resources

The URLs for data presented herein are as follows:

dbSNP, www.ncbi.nlm.nih.gov/projects/SNP/
SNP HiTLink software, http://www.dynacom.co.jp/u-tokyo.ac.jp/snphitlink/

Accession Numbers

The dbSNP accession numbers for the SNPs reported in this paper are ss252841181 and ss252841182.

References

1. Miyake, Y., Ichikawa, K., Shiose, Y., and Kawase, Y. (1989). Hereditary macular dystrophy without visible fundus abnormality. Am. J. Ophthalmol. *108*, 292–299.

Table 1. Disease-Linked Haplotypes in Families 1 and 2

| Probe Set ID | dbSNP rs ID | Position | Family 1 | | | | | Family 2 | |
| | | | Branch 1-1 | | Branch 1-2 | | | | |
			III-8	IV-9	IV-13	IV-18	IV-21	II-2	III-2
SNP_A-8338925	rs365309	9,064,350	(A)	(A)	A	A	B	A	A
SNP_A-8281994	rs1530483	9,065,671	B	B	B	B	B	B	B
SNP_A-8360926	rs10086673	10,342,727	B	B	(B)	B	B	(A)	A
SNP_A-2082488	rs9329223	10,369,164	A	A	A	A	A	(B)	B
SNP_A-2013182	rs6601491	10,453,427	B	B	B	B	B	(A)	A
RP1L1 p.Arg45Trp	c.133C>T	10,517,989	T	T	T	T	T	T	T
SNP_A-8345504	rs10097570	10,586,268	A	A	A	A	(A)	(B)	B
SNP_A-1790165	rs10111051	10,590,882	A	A	A	A	(A)	(B)	B
SNP_A-8587750	rs2163379	10,769,460	A	A	A	(A)	A	(B)	B
SNP_A-8500791	rs7460507	11,006,485	B	B	B	B	B	A	A
SNP_A-8525908	rs9772321	12,536,010	A	A	A	A	A	A	A
SNP_A-8283296	rs1021087	13,500,502	A	(A)	(A)	A	A	B	B
SNP_A-8441723	rs6987209	14,501,302	B	B	B	B	B	B	B
SNP_A-2044287	rs7818067	15,580,087	A	A	A	A	A	A	A
SNP_A-4273924	rs6992112	16,689,526	A	A	A	A	A	A	(A)
SNP_A-8447659	rs471041	17,707,836	B	B	B	B	B	B	B
SNP_A-8399664	rs2638658	18,713,620	A	(A)	(A)	A	A	(B)	B
SNP_A-4233785	rs2632841	18,716,063	B	B	(B)	B	A	B	B

Disease-linked haplotypes of the two patients (IV-9 and III-8) who are descendants from II-1 (branch 1-1 of family 1), the three patients (IV-13, IV-18, and IV-21) who are descendants from II-7 (branch 1-2 of family 1), and the two patients (II-2 and III-2) from family 2 are shown. Haplotypes are unequivocally determined, except those with brackets that are inferred to minimize the number of recombination events. Disease-linked haplotypes of the two branches of family 1 are the same, confirming that all affected individuals in family 1 share the same haplotype. Recombination events in the family was observed at rs365309 (telomeric boundary) and at rs2632841 (centromereic boundary). When disease haplotypes are compared between families 1 and 2, who share the p.Arg45Trp mutation in RP1L1 in common, disease-linked haplotypes flanking the RP1L1 locus are different between these families, suggesting that the p.Arg45Trp mutation originated independently.

2. Miyake, Y., Horiguchi, M., Tomita, N., Kondo, M., Tanikawa, A., Takahashi, H., Suzuki, S., and Terasaki, H. (1996). Occult macular dystrophy. Am. J. Ophthalmol. 122, 644–653.

3. Wildberger, H., Niemeyer, G., and Junghardt, A. (2003). Multi-focal electroretinogram (mfERG) in a family with occult macular dystrophy (OMD). Klin. Monatsbl. Augenheilkd. 220, 111–115.

4. Piao, C.H., Kondo, M., Tanikawa, A., Terasaki, H., and Miyake, Y. (2000). Multifocal electroretinogram in occult macular dystrophy. Invest. Ophthalmol. Vis. Sci. 41, 513–517.

5. Brockhurst, R.J., and Sandberg, M.A. (2007). Optical coherence tomography findings in occult macular dystrophy. Am. J. Ophthalmol. 143, 516–518.

6. Fukuda, Y., Nakahara, Y., Date, H., Takahashi, Y., Goto, J., Miyashita, A., Kuwano, R., Adachi, H., Nakamura, E., and Tsuji, S. (2009). SNP HiTLink: a high-throughput linkage analysis system employing dense SNP data. BMC Bioinfomatics 10, 121.

7. Gudbjartsson, D.F., Thorvaldsson, T., Kong, A., Gunnarsson, G., and Ingolfsdottir, A. (2005). Allegro version 2. Nat. Genet. 37, 1015–1016.

8. Yamashita, T., Liu, J., Gao, J., LeNoue, S., Wang, C., Kaminoh, J., Bowne, S.J., Sullivan, L.S., Daiger, S.P., Zhang, K., et al. (2009). Essential and synergistic roles of RP1 and RP1L1 in rod photoreceptor axoneme and retinitis pigmentosa. J. Neurosci. 29, 9748–9760.

9. Park, S.J., Woo, S.J., Park, K.H., Hwang, J.M., and Chung, H. (2010). Morphologic photoreceptor abnormality in occult macular dystrophy on spectral-domain optical coherence tomography. Invest. Ophthalmol. Vis. Sci. 51, 3673–3679.

10. Sisk, R.A., Berrocal, A.M., and Lam, B.L. (2010). Loss of foveal cone photoreceptor outer segments in occult macular dystrophy. Ophthalmic Surg Lasers Imaging 41, 1–3.

11. Conte, I., Lestingi, M., den Hollander, A., Alfano, G., Ziviello, C., Pugliese, M., Circolo, D., Caccioppoli, C., Ciccodicola, A., and Banfi, S. (2003). Identification and characterization of the retinitis pigmentosa 1-like1 gene (RP1L1): a novel candidate for retinal degenerations. Eur. J. Hum. Genet. 11, 155–162.

12. Bowne, S.J., Daiger, S.P., Malone, K.A., Heckenlively, J.R., Kennan, A., Humphries, P., Hughbanks-Wheaton, D., Birch, D.G., Liu, Q., Pierce, E.A., et al. (2003). Characterization of

Table 2. Summary of RP1L1 Mutations in Families with OMD

ID in Pedigree	Clinical Stage	Sex	Age at Diagnosis	Age at Onset in Estimation	Mutation	Best Corrected Visual Acuity (Right / Left)
1 III3	affected	F	81	50	c.362C>T	1.2 / 0.1
1 III4	affected	F	71	25	c.362C>T	0.4 / 0.5
1 III5	affected	M	74	30	c.362C>T	0.2 / 0.3
1 III8	affected	M	82	20	c.362C>T	0.2 / 0.2
1 IV1	unaffected	F	60	-	c.362C>T	1.2 / 1.2
1 IV9	affected	F	49	unknown	c.362C>T	1.2 / 1.2
1 IV12	affected	F	69	50	c.362C>T	0.1 / 0.07
1 IV13	affected	M	70	20	c.362C>T	0.1 / 0.1
1 IV14	affected	M	66	30	c.362C>T	0.2 / 0.3
1 IV18	affected	F	58	12	c.362C>T	0.1 / 0.1
1 IV21	affected	F	58	47	c.362C>T	0.1 / 0.4
1 V2	affected	M	20	13	c.362C>T	0.3 / 0.3
1 V3	affected	F	19	6	c.362C>T	0.2 / 0.15
2 II2	affected	M	69	unknown	c.362C>T	0.2 / 0.2
2 II4	unaffected	M	58	-	c.362C>T	1.0 / 1.0
2 II5	unaffected	M	55	-	c.362C>T	1.0 / 1.0
2 II8	affected	M	52	unknown	c.362C>T	0.2 / 0.3
2 III1	affected	M	23	23	c.362C>T	0.2 / 0.3
2 III2	affected	M	20	20	c.362C>T	0.3 /0.3
3 II1	affected	F	29	12	c.3107T>C	0.2 / 0.2
3 II3	affected	M	19	13	c.3107T>C	0.2 / 0.3
4 III3	affected	F	52	30	c.362C>T	0.15 / 0.15

Summary of individuals from autosomal OMD families 1–4, in whom p.Arg45Trp or p.Trp960Arg mutations of *RP1L1* were found. Three unaffected individuals at the age of 55–60 were found with the mutation. These individuals suggest a reduced penetrance of the mutation or a possible onset at a later age.

RP1L1, a highly polymorphic paralog of the retinitis pigmentosa 1 (RP1) gene, Mol. Vis. 9, 129–137.

13. Pierce, E.A., Quinn, T., Meehan, T., McGee, T.L., Berson, E.L., and Dryja, T.P. (1999). Mutations in a gene encoding a new oxygen-regulated photoreceptor protein cause dominant retinitis pigmentosa. Nat. Genet. 22, 248–254.

14. Sullivan, L.S., Heckenlively, J.R., Bowne, S.J., Zuo, J., Hide, W.A., Gal, A., Denton, M., Inglehearn, C.F., Blanton, S.H., and Daiger, S.P. (1999). Mutations in a novel retina-specific gene cause autosomal dominant retinitis pigmentosa. Nat. Genet. 22, 255–259.

15. Jacobson, S.G., Cideciyan, A.V., Iannaccone, A., Weleber, R.G., Fishman, G.A., Maguire, A.M., Affatigato, L.M., Bennett, J., Pierce, E.A., Danciger, M., et al. (2000). Disease expression of

RP1 mutations causing autosomal dominant retinitis pigmentosa. Invest. Ophthalmol. Vis. Sci. 41, 1898–1908.

16. Liu, Q., Lyubarsky, A., Skalet, J.H., Pugh, E.N., Jr., and Pierce, E.A. (2003). RP1 is required for the correct stacking of outer segment discs. Invest. Ophthalmol. Vis. Sci. 44, 4171–4183.

17. Liu, Q., Zuo, J., and Pierce, E.A. (2004). The retinitis pigmentosa 1 protein is a photoreceptor microtubule-associated protein. J. Neurosci. 24, 6427–6436.

18. Gleeson, J.G., Allen, K.M., Fox, J.W., Lamperti, E.D., Berkovic, S., Scheffer, I., Cooper, E.C., Dobyns, W.B., Minnerath, S.R., Ross, M.E., and Walsh, C.A. (1998). Doublecortin, a brain-specific gene mutated in human X-linked lissencephaly and double cortex syndrome, encodes a putative signaling protein. Cell 92, 63–72.

Dominant Mutations in *RP1L1*

Are Responsible for Occult Macular Dystrophy

Masakazu Akahori, Kazushige Tsunoda, Yozo Miyake, Yoko Fukuda, Hiroyuki Ishiura, Shoji Tsuji, Tomoaki Usui, Tetsuhisa Hatase, Makoto Nakamura, Hisao Ohde, Takeshi 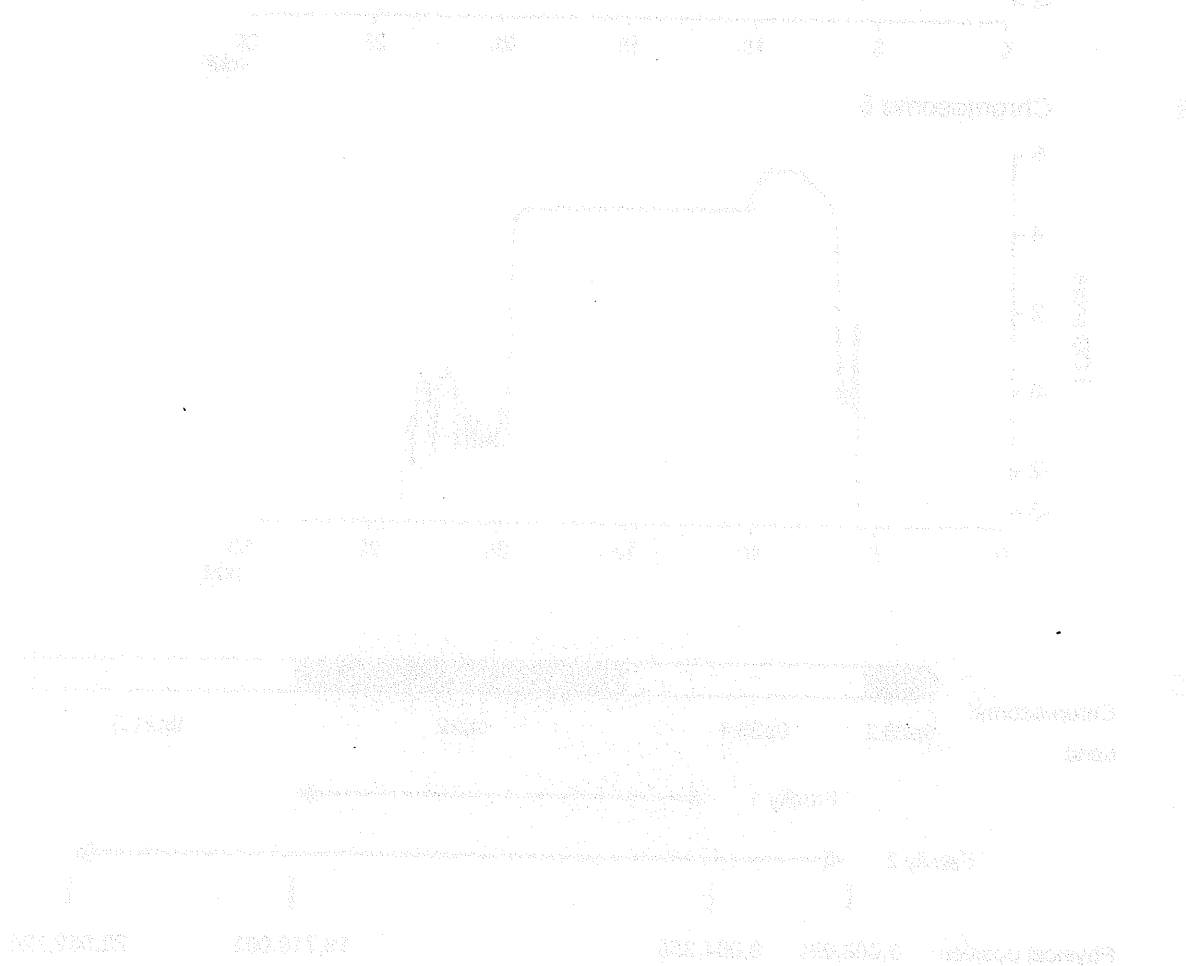Itabashi, Haru Okamoto, Yuichiro Takada, and Takeshi Iwata